Korean J. Chem. Eng., **28**(6), 1364-1371 (2011)
DOI: 10.1007/s11814-010-0528-5

Improved performance of Mo-V-Te-Nb-O_x catalysts prepared from a solution containing drying control chemical additives in propane oxidation to acrylic acid

Sang Seop Kum, Yoon Sik Park, and Sang Heup Moon†

School of Chemical & Biological Engineering and Institute of Chemical Processes,
Seoul National University, Seoul 151-744, Korea
(*Received 2 December 2010 • accepted 28 December 2010*)

Abstract−$Mo_{1.0}V_{0.4}Te_{0.25}Nb_{0.24}O_x$ catalyst was prepared by hydrothermal synthesis in a solution containing a drying control chemical additive (DCCA) such as propionic acid (PA) or formamide (FA). The performance of the prepared catalysts in propane oxidation for producing acrylic acid (AA) was improved because the catalyst showed an increase in both the activity and AA selectivity. The activity was increased due to an increase in the surface area and in the oxygen mobility. The AA selectivity was increased due to a decrease in the number of acidic sites, which were responsible for the unselective and deep oxidation of intermediates. The catalyst performance was degraded when excess amounts of DCCA were used in the preparation step because the surface area decreased, due to the residues of DCCA, and the surface density of acidic sites increased.

Key words: $MoVTeNbO_x$, Propane Oxidation, Acrylic Acid, Drying Control Chemical Additive

INTRODUCTION

Replacing propylene with propane as a feed of selective oxidation process to produce acrylic acid (AA) is an important challenge in catalysis research [1-4]. One of candidate catalysts for the process is the Mo-V-Te-Nb-O_x system containing two major phases: an orthorhombic M1 phase, taking the major role of activating paraffin by surface V^{5+} species, and a hexagonal M2 phase, serving as a co-catalyst or a mop-up phase converting propylene to acrolein [5-10]. The propylene species are known to be produced on the M1 phase and transferred to M2 sites during the reaction.

There were attempts to increase the surface area of the Mo-V-Te-Nb-O_x catalyst using surfactants such as cetyl trimethylammonium bromide or supports, but the prepared catalysts exhibited low productivity of AA per unit surface area [11,12]. Jo et al. [13] reported that both the surface area and the activity of Bi-Mo-Co-Fe-K-O catalysts for propylene oxidation could be increased when the catalysts were synthesized in a solution containing drying control chemical additives (DCCA). The DCCA is an organic material commonly used in a sol-gel process to make the growth rates of crystallites constant and to reduce the interfacial tension between sol and gel phases. Accordingly, the DCCA contributed to an increase in the surface area of prepared catalysts by forming small, uniform pores and by suppressing pore cracks in the drying step [14,15].

In this study, we prepared Mo-V-Te-Nb-O_x particles by a hydrothermal method from a solution containing DCCA, and examined their reaction and surface properties as they changed with the types and amounts of the DCCA.

†To whom correspondence should be addressed.
E-mail: shmoon@surf.snu.ac.kr

EXPERIMENTAL

1. Catalyst Preparation

The DCCA-added Mo-V-Te-Nb-O_x catalysts with nominal atomic ratios, Mo/V/Te/Nb=1/0.4/0.25/0.24, were prepared by hydrothermal synthesis as previously reported [16-29]. Ammonium paramolybdate (4.5 g) and telluric acid (1.405 g) were dissolved in 20 ml of distilled water. A second or a third solution was prepared by dissolving hydrated vanadyl sulfate (2.61 g) or hydrated niobium oxalate (1.835 g) in 10 ml of distilled water. Propionic acid (PA) or formamide (FA) was added as a DCCA to the first solution with stirring. The second solution containing V was added to the first solution containing Mo, Te and DCCA, and the resulting solution was stirred for 5 min. The third solution containing Nb was finally added to the above mixed solution, and the resulting slurry was stirred for 10 min. All operations, including preparation and stirring of the solution, were performed at 75 °C. The slurry was introduced into a stainless-steel autoclave that was sealed and heated at 175 °C for 6 h after nitrogen bubbling for 5 min. The dark blue powder obtained was washed with distilled water and dried at 110 °C for 12 h. The dried powder was sequentially heat-treated at 600 °C in nitrogen flow for 2 h. All samples modified with DCCA will be indexed as "DCCA X", in which X denotes the amount of added DCCA in the molar ratio of DCCA over Mo.

2. Reaction

Propane oxidation was conducted using 0.1 g of catalyst in a stainless-steel tubular reactor (ID: 4.5 mm) at temperatures between 350 °C and 400 °C. The molar fractions of feed components with a fixed space velocity of 1,000 h^{-1} were propane/O_2/N_2/H_2O=0.08/0.21/0.33/0.38, respectively. A gas line connecting the reactor to a gas chromatograph was maintained at 170 °C during the reaction tests

to prevent possible condensation of reaction products inside the line. A multi-position valve connected to eight parallel reactors changed the analyzing channel in sequence such that the tests were made simultaneously in a short period.

The gas chromatograph was equipped with two capillary columns connected in parallel. One was a sequential column consisting of CP-Al_2O_3/KCL (Varian) and SOLGEL WAX (SGE), which was connected with a flame ionization detector (FID), for the separation and analysis of hydrocarbons. The other was a 60/80 CARBOXEN 1000 (Supelco) column that was connected with a thermal conductivity detector (TCD) for the separation and analysis of N_2, O_2, CO and CO_2. The conversion of propane and the selectivity for the production of specific products were calculated based on carbon balance.

3. Characterization

3-1. Surface Area and Crystallite Structure

The BET surface areas and pore volumes of the sample catalysts were measured by using ASAP 2010 (Micromeritics Co.). All sample catalysts were degassed at 200 °C for 2 h to remove physically adsorbed water from the surface prior to the adsorption of N_2.

Crystalline phases of the sample catalysts were analyzed by X-ray diffraction (XRD) using M18XHF-SRA (MAC Science Co.), which was operated with a Cu Kα source at 40 kV and 200 mA. The scan rate was 5°/min.

A field emission scanning-electron microscope (FE SEM, model SUPRA 55VP, Carl Zeiss Ltd.) was used to obtain the real image of prepared crystallites. Samples were coated with a platinum layer prior to the observations.

3-2. Oxygen Mobility, Surface Residues and Acidic Sites

The mobility of oxygen that makes up the lattice oxygen consumed in the oxidation process was analyzed by the temperature-programmed oxidation (TPO) of the catalyst. Prior to the TPO experiments, the catalyst was used in propane oxidation at 400 °C for 3 h without supplying O_2 in the feed. In this way, the catalyst was partially reduced by consuming its lattice oxygen for oxidizing propane. After the reduced catalyst was placed in JP/Bel-Cat (Bel Japan Inc.), a stream of 5% O_2 and 95% Ar was introduced to a reactor containing the sample catalyst. Temperature was then raised from 20 °C to 550 °C at a heating rate of 10 °C/min. The amounts of O_2 consumed in the stream were measured with a TCD.

The amounts of residues on the prepared catalysts, which could originate from DCCA that had been added in excess amounts, were analyzed by temperature-programmed desorption (TPD). The DCCA-added catalyst was heated from 20 °C to 600 °C at a rate of 10 °C/min in flowing He, while the species desorbing from the catalyst were monitored by signals of a mass spectrometer HAL201-RC (Hiden Co.) at m/e=74, 29, 27 for PA and at m/e=45, 44, 28 for FA.

NH_3-TPD experiments were carried out using JP/Bel-Cat (Bel Japan Inc.) to estimate the amounts of acidic sites on the catalyst surface. All samples were pre-treated at 150 °C for 1 h in He and then cooled to room temperature. For the TPD, pulses of NH_3 were introduced to the catalyst surface for adsorption, which was followed by purging with He for 1 h. Then, the sample catalyst was heated from 20 °C to 650 °C at a rate of 10 °C/min and the desorbed gas was analyzed for NH_3 using a TCD.

RESULTS

1. Oxidation of Propane

Fig. 1(a), which shows the conversions of propane obtained by

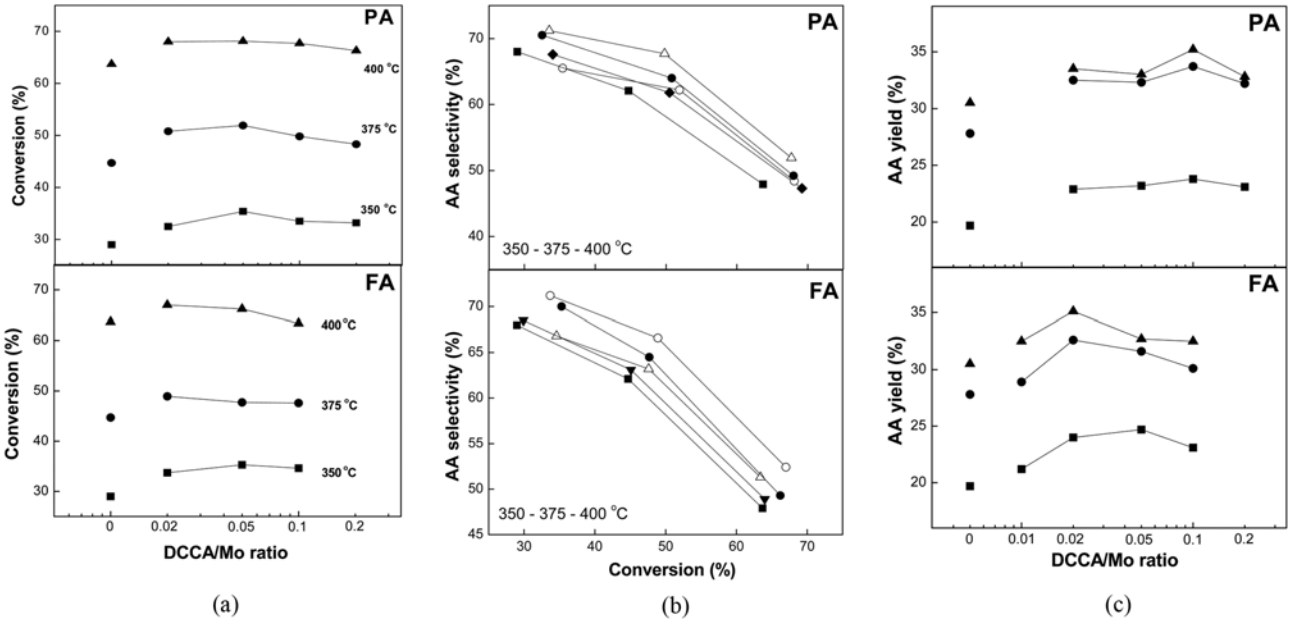

Fig. 1. (a) Propane conversions in propane oxidation, obtained using sample catalysts. The X-axis is in log scale. Reaction temperatures are (■) 350 °C, (●) 375 °C, and (▲) 400 °C. Catalyst amount=0.1 g; space velocity=1,000 h^{-1}. Propane : oxygen : nitrogen : water= 0.08 : 0.21 : 0.33 : 0.38 (molar fractions). (b) Selectivity for acrylic acid in propane oxidation, obtained using sample catalysts. The DCCA/Mo molar ratios are (■) 0, (▼) 0.01, (○) 0.02, (●) 0.05, (△) 0.1, and (◆) 0.2. Other conditions are the same as in Fig. 1(a). (c) The acrylic-acid (AA) yield in propane oxidation, obtained using sample catalysts. Reaction temperatures are (■) 350 °C, (●) 375 °C, and (▲) 400 °C. Other conditions are the same as in Fig. 1(a).

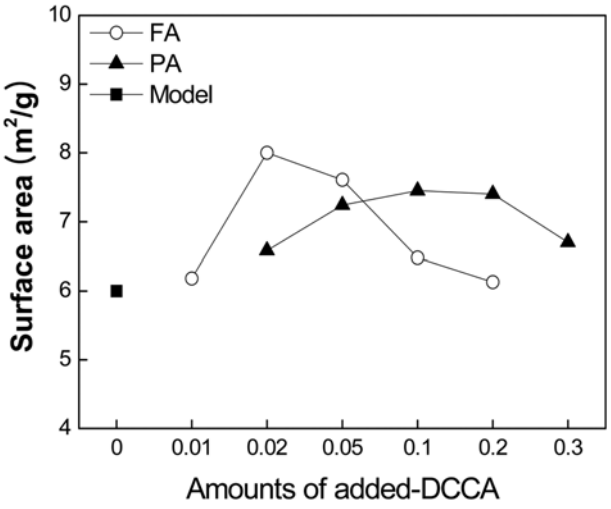

Fig. 2. Change in the surface areas of sample catalysts with the amounts of added DCCA. Samples are (■) Model, (▲) PA-added, and (○) FA-added catalysts.

using the PA- and FA-added catalysts at different reaction temperatures, indicates that the activity was enhanced by the DCCA addition and showed a maximum when the DCCA/Mo ratios were 0.02-0.05. Fig. 1(b) shows that the AA selectivity, which decreased at high conversions, was also enhanced by the DCCA addition. Consequently, the AA yield, obtained by multiplying the conversion with the selectivity, showed a maximum when the DCCA/Mo ratio was 0.1 for PA and 0.02 for FA, respectively (Fig. 1(c)). The enhancement in the AA yield was largely due to an increase in the activity in the case of the PA-added catalyst but it was due to an increase in the selectivity in the case of the FA-added catalyst.

2. Characterization

2-1. Surface Area

The BET surface areas of the catalysts increased with an increase in the amounts of added DCCA until a maximum was observed when the DCCA/Mo ratio was 0.1 for PA (7.5 m^2/g) and 0.02 for FA (8 m^2/g), respectively (Fig. 2).

The pore volume of the catalysts also changed with the amounts of added DCCA (the results are not shown here), showing a trend similar to that of surface area. On the other hand, the pore size distribution was similar among the prepared catalysts, regardless of the types and amounts of added DCCA. Accordingly, it was concluded that the surface area was increased due to the generation of new pores of the same structure.

2-2. Crystallite Phase

The XRD spectra of the prepared catalysts, shown in Fig. 3, represent three crystallite phases: $Mo_{5-X}(V/Nb)_XO_{14}$ (2θ=7.7, 8.7, 14.0, 22.1, 23.3, 24.9, 29.7, 31.5, 32.4 and 33.5), $Te_2M_{20}O_{57}$ (M1: 2θ= 7.7, 9.0, 22.1, 26.2, 26.8, 27.3, 29.2, and 35.4), and $Te_{0.33}MO_{3.33}$ (M2: 2θ=22.1, 28.2, 36.2, 45.2, and 50.0), where M in the latter two phases indicates either Mo, V, or Nb [30-33]. The intensities of two peaks representing M1 (29.2°) and M2 (28.2°) phases, and the intensity ratios of the two peaks, M1 (29.2°)/ M2 (28.2°), are presented in Table 1. The ratios of the two peaks remained nearly constant (0.52-0.55), independent of the amounts of added PA, but increased (0.58-0.91) with the amounts of added FA. The trend of the FA-added

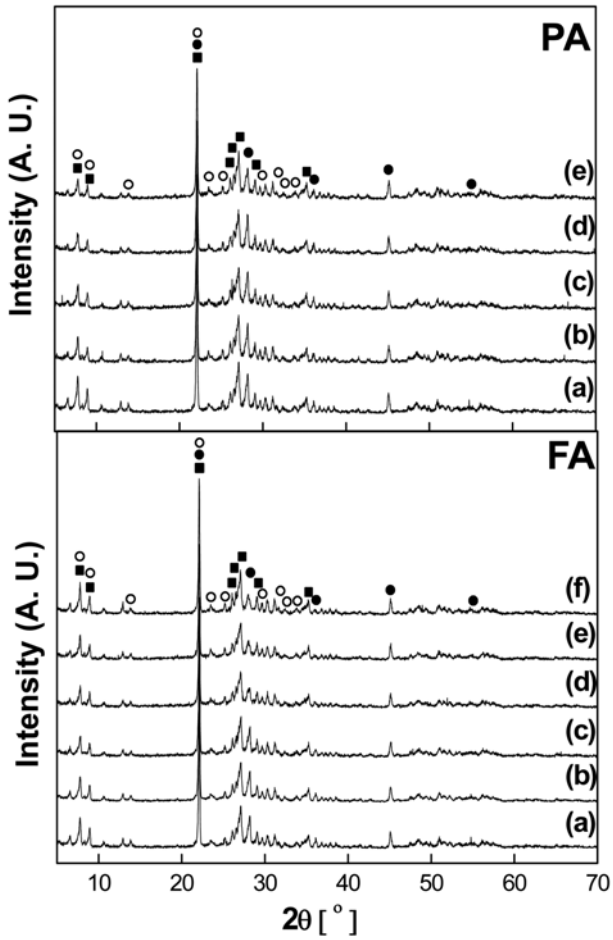

Fig. 3. X-ray diffraction patterns of sample catalysts. (a) Model, (b) 0.05, (c) 0.1, (d) 0.2, and (e) 0.3 for PA-added catalyst, (a) Model, (b) 0.01, (c) 0.02, (d) 0.05, (e) 0.1, and (f) 0.2 for FA-added catalyst. Individual crystallite phases are represented by the following characteristic peaks [30-33]. ○: $Mo_{5-X}(V/Nb)_XO_{14}$ (2θ=7.7, 8.7, 14.0, 22.1, 23.3, 24.9, 29.7, 31.5, 32.4 and 33.5°), ■: $Te_2M_{20}O_{57}$ (M1: 2θ=7.7, 9.0, 22.1, 26.2, 26.8, 27.3, 29.2 and 35.4°), ●: $Te_{0.33}MO_{3.33}$ (M2: 2θ= 22.1, 28.2, 36.2, 45.2 and 50.0°).

Table 1. The intensities of characteristic XRD peaks representing individual crystallite phases of sample catalysts

Catalyst	M1 (29.2°)	M2 (28.2°)	M1 (29.2°)/M2 (28.2°)
Model	11	23	0.48
PA 0.05	14	25	0.54
PA 0.1	15	28	0.55
PA 0.2	14	27	0.52
FA 0.02	14	24	0.58
FA 0.05	14	17	0.78
FA 0.1	15	16	0.91

catalysts was observed largely because the intensity of M2 peak (28.2°) decreased at excessive amounts of FA. It is noteworthy that FA is more basic than water. Oliver et al. [34], who studied the morphology and crystallite structure of Mo-V-Te-Nb-O_x catalysts prepared by a slurry method at different pH, observed that a part of Te was

lost during heat-treatment when the catalysts were prepared at pH higher than an optimum value. As Te is located at the center of a hexagonal channel in M2 phase, the loss of Te can suppress the formation of the M2 phase.

In both cases of the DCCA addition, the peak intensity ratio was higher than in the case of the model catalyst (0.48), indicating that the relative amounts of M1 phase with respect to M2 phase were increased by the DCCA addition.

2-3. FE-SEM

The crystallites of DCCA-added catalysts were observed by FE-SEM, as shown in Fig. 4. The stick-shaped crystallites of the model catalyst (Fig. 4(a)), which represent the orthorhombic M1 phase [35], are about 600-800 nm long as indicated by boxes in the figure. The length of the M1 phase of FA 0.02 catalyst (Fig. 4(b)), which was in the range of 300-500 nm, was clearly shorter than that of model catalyst. The length was even shorter for FA 0.2 catalyst (Fig. 4(c)), in which case the stick-shaped crystallites longer than 500 nm were hardly observed. A similar trend in the size of M1 crystallites was observed with PA-added catalysts. The stick-shaped crystallites of PA 0.1 catalyst were in the uniform size range of 400-500 nm, and those of PA 0.3 catalyst were smaller than 400 nm (Figs. 4(d) and 4(e)). Accordingly, it can be concluded based on the above observations that the size, particularly the length, of M1 crystallites was decreased by the DCCA addition.

2-4. Oxygen Mobility

Fig. 5 shows the TPO profiles of sample catalysts, which were partially depleted of the lattice oxygen species after they had been used for propane oxidation in an O_2-free propane stream. All the catalysts showed two major peaks at temperatures below 500 °C, which represent oxygen required for replenishing the oxygen spe-

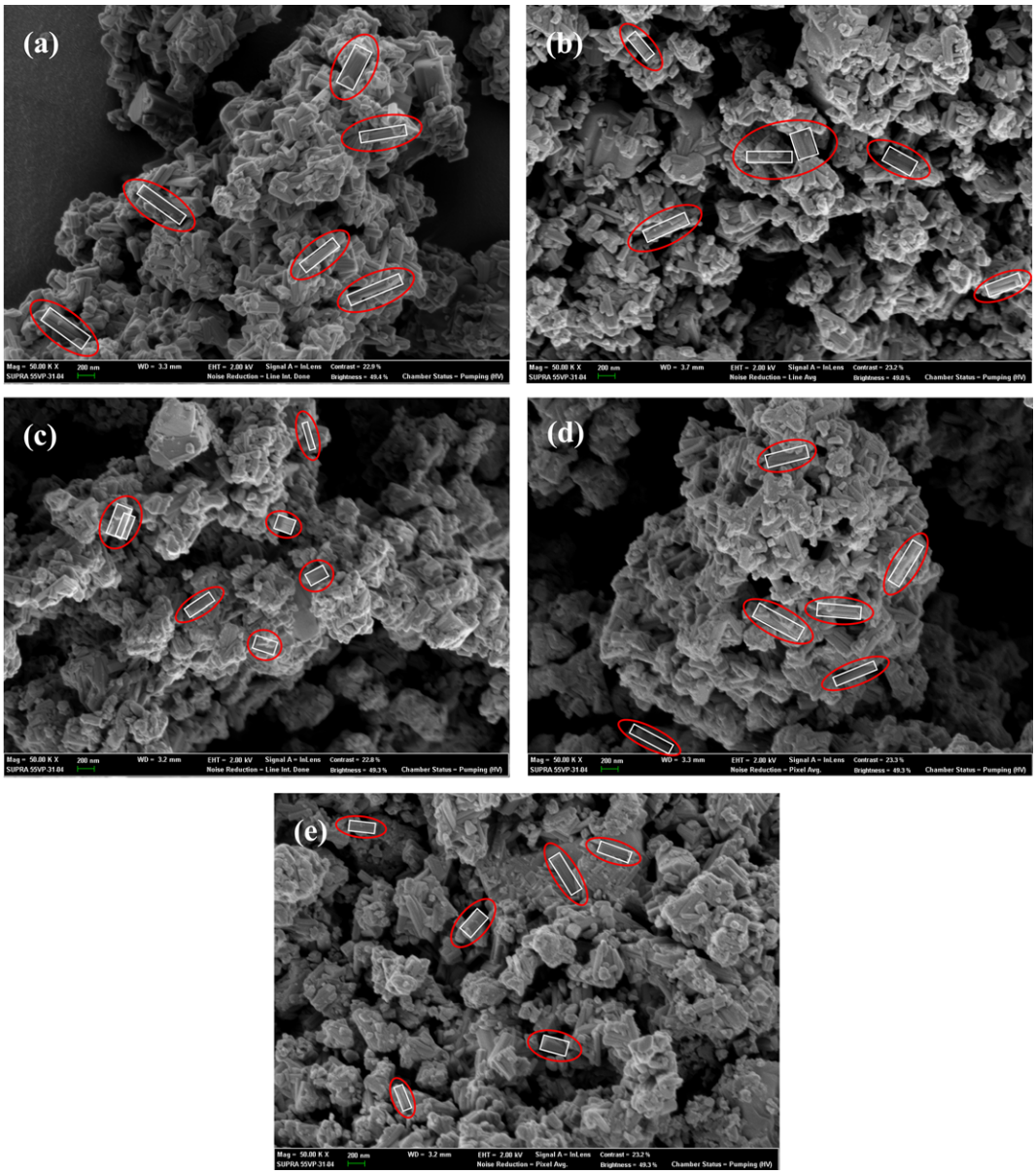

Fig. 4. SEM images of prepared catalysts. (a) Model, (b) FA 0.02, (c) FA 0.2, (d) PA 0.1, and (e) PA 0.3. The highlighted boxes indicate M1 crystallites [50,000 magnification].

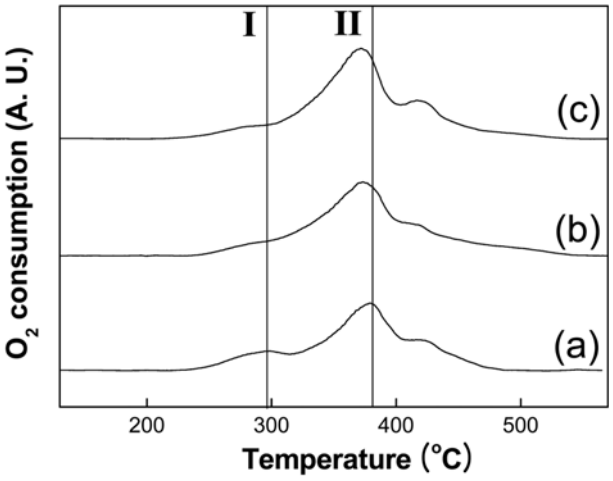

Fig. 5. TPO results obtained using sample catalysts. (a) Model, (b) FA 0.02, and (c) PA 0.1.

cies that were consumed in the oxidation process. That is, a peak observed at about 300 °C (Peak I) is attributed to the oxygen species present on the catalyst surface, while the one appearing near 400 °C (peak II) is due to the lattice oxygen in the catalyst structure [36-41]. It is noteworthy in Fig. 5 that peaks I and II were shifted to lower temperatures due to the DCCA addition compared with the case of model catalyst. In particular, peak II was shifted by as large as 10 °C in both cases of FA 0.02 and PA 0.1, indicating that the mobility of the lattice oxygen was enhanced by the DCCA addition.

Fig. 5 also shows that the intensity of peak II increased with the DCCA addition, by about 1.15 and 1.1-fold for FA 0.02 and PA 0.1, respectively. This result agrees with the increased oxygen mobility of DCCA-added catalysts, which will simultaneously increase the amounts of oxygen consumed during propane oxidation.

2-5. Residue Analysis

The results of TPD experiments to monitor the species originating from either PA 0.3 or FA 0.1 at elevated temperatures are shown in Fig. 6. The sample catalysts were selected among those containing large amounts of DCCA because the mass signals in the TPD were weak. The results indicate that FA, represented by a mass signal at m/e=44, was decomposed at higher temperatures than PA, represented by a signal at m/e=29. Accordingly, the DCCA residues are expected to be deposited in larger amounts on the FA-added catalysts than on the PA-added ones.

2-6. NH_3 TPD

The results of NH_3-TPD from the catalysts (Fig. 7) show two peaks, an intensive one centered at about 200 °C and the other appearing as a broad shoulder at above 300 °C, representing the acidic sites of different strength [42,43]. The DCCA addition did not affect the position of the TPD peaks, which represented the acidic strength, but decreased the intensity of the peaks, which represented the amounts of the acidic sites. In particular, the intensity of peak II decreased to greater extents than that of peak I in both cases of the PA- and FA-addition, which indicated that the DCCA addition preferentially decreased the amounts of relatively strong acidic sites. The quantitative data of the above results are summarized in Table 2. Between

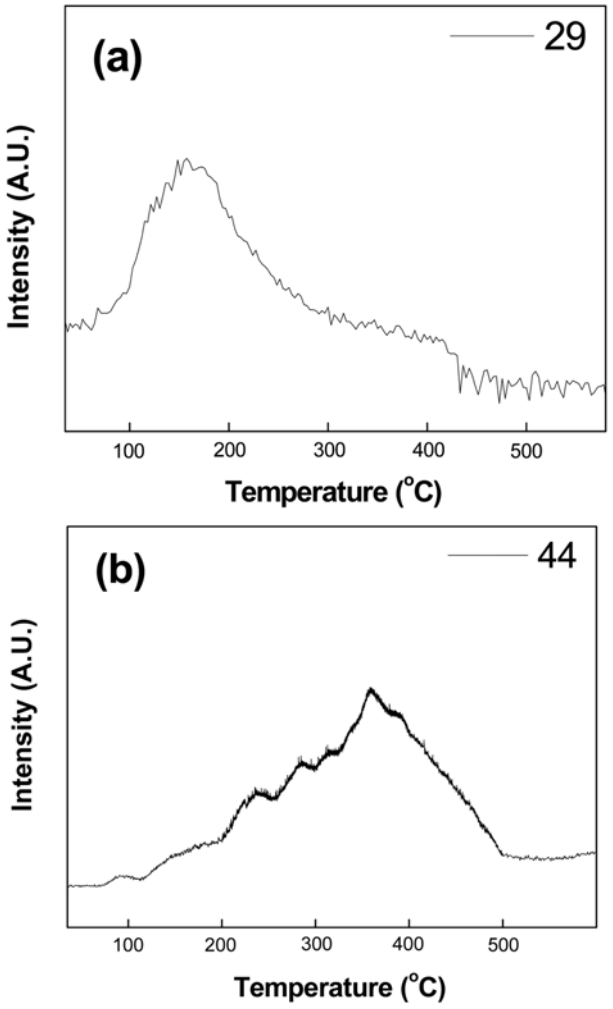

Fig. 6. Mass signals of (a) PA (represented by m/e=29) and (b) FA (represented by m/e=44) in the TPD experiments using PA 0.3 and FA 0.1, respectively.

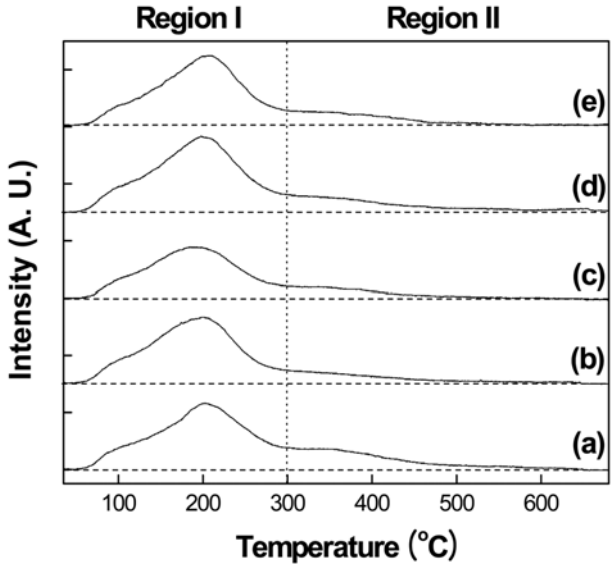

Fig. 7. TPD of NH_3 from sample catalysts containing different amounts of DCCA. (a) Model, (b) PA 0.1, (c) PA 0.3, (d) FA 0.02, and (e) FA 0.1.

Table 2. The amounts of ammonia desorbed from sample catalysts during NH_3 TPD experiments (Fig. 7)

Catalyst	Model	PA 0.1	PA 0.3	FA 0.02	FA 0.1
Area of NH_3-TPD peaks	205	178	162	203	183
Surface area (m^2/g)	6	7.5	6.7	8	6.5
Area of NH_3-TPD peaks/surface area	34.2	23.7	24.2	25.3	28
Fractional amounts (%) of acidic sites represented by a peak in region II (Fig. 7)	35	21	22	25	24

PA and FA, PA seems to be slightly more effective for decreasing the acid amounts than the FA, but a definite conclusion should be retained due to errors involved in the estimation of the acid amounts.

DISCUSSION

1. Surface Area of DCCA-added Catalyst

According to Fig. 2, catalysts prepared from a solution containing DCCA had higher surface areas than the model catalyst. This result can be explained based on two characteristics of DCCA.

One is that DCCA lowered the interfacial tension between sol and gel phases that were formed in the catalyst preparation process to allow the precipitation of relatively small particles, leading to an increase in the catalyst surface area.

The other is the high viscosity of DCCA compared with water, which decreased the rates of hydrothermal reaction [44-46] and eventually the growth of the crystallites of M1 phase in the prepared catalysts, as observed in Fig. 4. The suppression of the crystallite growth was more significant in the case of using FA, which had a viscosity of 4.3 mPa·s, than in the case of using PA, which had a viscosity of 1.52 mPa·s. The viscosity of PA was similar to that of water but its acidic property might have affected the growth of crystallites, as reported in other studies [47-51].

The catalyst surface area was eventually lowered when DCCA was added in excessive amounts, i.e., greater than 0.1 (PA) and 0.02 (FA), because the residues of added DCCA accumulated on the catalyst surface. The accumulation of the residues was more significant with FA than with PA, as supported by the results of the residue-monitoring tests shown in Fig. 6. Consequently, the surface area started to decrease with smaller amounts of added FA than in the case of PA.

2. Activity for Propane Oxidation

The activity of Mo-V-Te-Nb-O_x catalyst for propane oxidation increased with the DCCA addition, which can be explained based on three observations made in this study.

The first explanation is an increase in the surface area. The amount of added DCCA that allowed the highest surface area agreed with that allowed the optimum activity. Although changes in the activity were smaller than those in surface areas, which was obtained because the reaction tests were made in an integral reaction scheme, it is obvious that an increase in the surface area contributed to the improvement of activity.

The second one is enhancement in oxygen mobility. Fig. 5 indicates that the TPO peaks, particularly peak II that originated from the replenishment of consumed lattice oxygen, were shifted to lower temperatures in the cases of PA 0.1 and FA 0.02 compared with the case of model catalyst. Accordingly, lattice oxygen consumed by the reaction was replenished more efficiently in the former catalysts than in the latter. The reason for the enhanced oxygen mobility of the DCCA-added catalysts is believed to be the reduced crystallite size of M1 phase in the catalysts (Fig. 4), which will decrease the distance for oxygen migration in the lattice.

The third explanation of the activity improvement can be made considering changes in the relative amount of M1 compared to that of M2 phase. The relative amounts of M1 increased in the DCCA-added catalysts, particularly in PA 0.1 and FA 0.02 catalysts which showed the maximum conversions. The above scenario is in accordance with the work of Tu [52], who suggested that a high M1/M2 ratio was beneficial to the catalytic activity for propane oxidation because the reaction proceeded largely on the M1 phase.

The major reason for the degradation of activity with the amounts of added DCCA greater than the optimum, i.e., 0.1 (PA) and 0.02 (FA), is believed to be a decrease in the surface area (Table 2) by coverage with the surface residues (Fig. 6). In the case of FA-added catalyst, a significant decrease in the amounts of M2 phase will reduce the rates of propane oxidation because M2 is responsible for transferring lattice oxygen to the M1 phase [5,42,53].

3. Selectivity for Acrylic Acid

The propane oxidation pathway consists of two major paths, as described in Fig. 8 [3,54,55]. One is the main path starting from propane via propylene to acrolein and AA. The other is a side reaction via 2-propanol to produce acetone and acetic acid, which are the precursors of CO and CO_2. 2-propanol or acetone can be produced from propylene on acidic sites as well [55-57].

The AA selectivity of the catalysts increased with the DCCA addition, showing a maximum at the PA/Mo ratios of 0.1 and FA/Mo ratios of 0.02 (Fig. 1(b)). The enhancement in the AA selectivity by the DCCA addition can be explained by the following two reasons. One, reason is a decrease in the amount of acidic sites. According to Table 2, the total amounts of acidic sites, represented by the area of NH_3-TPD peaks, decreased even when the surface areas increased with the DCCA addition. Acidic sites in Mo-V-Te-Nb-O_x catalysts are known to promote side reactions leading to by-products, such as acetone, acetic acid and carbon oxides [2,58-60].

The DCCA addition preferentially decreased the amounts of strong

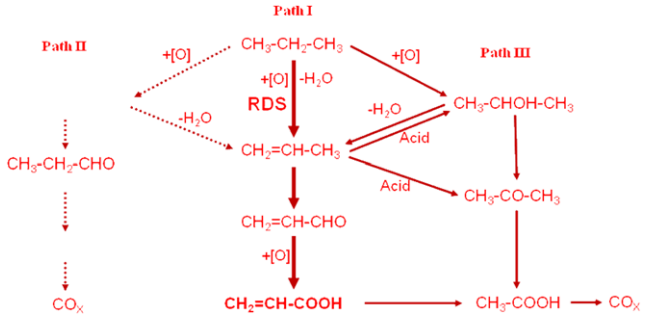

Fig. 8. Reaction pathways in propane oxidation [55].

acidic sites, represented by peak II (Fig. 7 and Table 2), which may include nucleophilic Lewis acid sites that favor the cracking of the C-C bond of propane to induce unselective deep oxidation [2,61,62], and Brønsted acid sites that are responsible for the conversion of propylene to undesired products, such as acetone and acetic acid [63,64]. A decrease in the number of the strong acidic sites indicates the suppression of side reactions leading to CO and CO_2. In conclusion, the AA selectivity of the DCCA-added catalysts increased due to a decrease in the amounts of acidic sites, particularly the strong acid sites.

The other reason for the selectivity improvement can be the promotion of the lattice-oxygen migration between M1 and M2 phases due to the reduced size of crystallites. Fine crystallites packed as close neighbors (shown in Fig. 4) will allow easy migration of oxygen between the two phases, which will eventually improve the ethylene selectivity.

The AA selectivity was decreased when the amounts of added FA and PA were greater than 0.02 and 0.1, respectively, which can be explained as follows.

Small-size crystallites formed on PA 0.3 and FA 0.2 catalysts must be densely packed and simultaneously contaminated with the surface residues, within a small space, which will hamper the quick diffusion of desorbed AA to outside the catalyst particles. In addition, a significantly high ratio of M1/M2 phases (Table 1) for FA-added catalyst is expected to depress the selectivity because the M2 phase is responsible for the selective oxidation of propylene that has been produced on and migrated from the M1 phase. It has been reported that the balanced ratio of M1/M2 phases is a key factor for the selective oxidation of propane [52,53,64-68].

CONCLUSIONS

The activity and selectivity of a hydrothermally-synthesized $Mo_{1.0}V_{0.4}Te_{0.25}Nb_{0.24}O_x$ catalyst in the partial oxidation of propane to acrylic acid were improved when the catalyst was prepared from a solution containing DCCA such as propionic acid and formamide.

The activity was promoted because the surface area of the catalyst was increased by the DCCA addition. The formation of smaller M1 and M2 crystallites, which allowed the enhanced oxygen mobility in the crystallites, also contributed to the increased activity.

The AA selectivity increased in the DCCA-added catalysts, largely due to a decrease in the amounts of acidic sites, particularly strong acidic sites. Overall, the AA yield was improved by 15.5% and 15% for PA 0.1 and FA 0.02 catalysts compared to the case of model catalyst.

The catalyst performance was degraded when the amounts of added DCCA were excessive because the surface area decreased and the number of acidic sites per surface area increased.

ACKNOWLEDGEMENT

This work was supported by Brain Korea 21 (BK 21) project and LG Chemical Co.

REFERENCES

1. M. M. Lin, *Appl. Catal. A*, **207**, 1 (2001).
2. Y. Moro-oka and W. Ueda, *Adv. Catal.*, **40**, 233 (1994).
3. M. Lin, T. B. Desai, F. W. Kaiser and P. D. Klugherz, *Catal. Today*, **61**, 223 (2000).
4. M. Ai, *Catal. Today*, **101**, 389 (1986).
5. B. Deniau, J. M. M. Millet, S. Loridant, N. Christin and J. L. Dubois, *J. Catal*., **260**, 30 (2008).
6. E. Balcells, F. Borgmeier, I. Griβtede, H.-G. Lintz and F. Rosowski, *Appl. Catal. A*, **266**, 211 (2004).
7. P. Botella, E. García-González, J. M. L. Nieto and J. M. González-Calbet, *Solid State Sci.*, **7**, 507 (2005).
8. J. M. L. Nieto, P. Botella, B. Solsona and J. M. Oliver, *Catal. Today*, **81**, 87 (2003).
9. B. Zhu, H. Li, W. Yang and L. Lin, *Catal. Today*, **93–95**, 229 (2004).
10. H. Tsuji, K. Oshima and Y. Koyasu, *Chem. Mater.*, **15**, 2112 (2003).
11. X. Yi, X. Sun, X. Zhang, C. Huang, W. Weng and H. Wan, *Catal. Comm.*, **10**, 1591 (2009).
12. M. Florea, A.-S. Mamede, P. Eloy, V. I. Parvulescu and E. M. Gaigneaux, *Catal. Today*, **112**, 139 (2006).
13. B. Y. Jo, E. J. Kim and S. H. Moon, *Appl. Catal. A*, **332**, 257 (2007).
14. D. R. Ulrich, *J. Non-Cryst. Solids*, **100**, 174 (1988).
15. D. M. Smith, R. Desphande, C. J. Brinker, in M. J. Hampden-Smith, W. G. Klemperer and C. J. Brinker, *Mater. Res. Soc.*, **271**, 553 (1992).
16. D. Vitry, Y. Morikawa, J. L. Dubois and W. Ueda, *Appl. Catal. A*, **251**, 411 (2003).
17. X. J. Yang, R. M. Feng, W. J. Ji and C. T. Au, *J. Catal*., **253**, 57 (2003).
18. J. M. Oliver, J. M. López Nieto and P. Botella, *Catal. Today*, **96**, 241 (2004).
19. R. M. Feng, X. J. Yang, W. J. Ji, H. Y. Zhu, X. D. Gu, Y. Chen, S. Han and H. Hibst, *J. Mol. Catal. A*, **267**, 245 (2007).
20. K. Oshihara, T. Hisano and W. Ueda, *Top. Catal*., **15**, 153 (2001).
21. P. Botella, J. M. López Nieto, A. Martínez-Arias and B. Solsona, *Catal. Lett*., **74**, 149 (2001).
22. P. Botella, J. M. López Nieto, B. Solsona, A. Mifsud and F. Márquez, *J. Catal*., **209**, 445 (2002).
23. A. Celaya Sanfiz, T. W. Hansen, F. Girgsdies, O. Timpe, E. Rödel, T. Ressler, A. Trunschke and R. Schlögl, *Top. Catal*., **59**, 19 (2008).
24. F. Ivars, B. Solsona, S. Hernández and J. M. López Nieto, *Catal. Today*, **149**, 260 (2010).
25. H. Murayama, D. Vitry, W. Ueda, G. Fuchs, M. Anne and J. L. Dubois, *Appl. Catal. A*, **318**, 137 (2007).
26. P. Beato, A. Blume, F. Girgsdies, R. E. Jentoft, R. Schlögl, O. Timpe, A. Trunschke, G. Weinberg, Q. Basher, F. A. Hamid, S. B. A. Hamid, E. Omar and L. Mohd Salim, *Appl. Catal. A*, **307**, 137 (2006).
27. Q. Xie, L. Chen, W. Weng and H. Wan, *J. Mol. Catal. A*, **240**, 191 (2005).
28. N. R. Shiju and V. V. Guliants, *Catal. Comm*., **9**, 2253 (2008).
29. N. R. Shiju and V. V. Guliants, *Appl. Catal. A*, **356**, 1 (2009).
30. K. Bruckman and J. Haber, *Proceedings of the 10th International Congress on Catalysis*, Budapest, Hungary, **741** (1993).
31. F. Cavani, M. Koutyrev and F. Trifiro, *Catal. Today*, **24**, 365 (1995).
32. G. Centi and F. Trifiro, *Proceedings of Conference on Catalysis of Science and Technology*, Tokyo, **225** (1991).
33. W. Ueda and Y. Suzuki, *Chem. Lett.*, **24**, 541 (1995).
34. J. M. Oliver, J. M. López Nieto, P. Botella and A. Mifsud, *Appl. Catal. A*, **257**, 67 (2004).
35. A. Celaya Sanfiz, T. W. Hansen, F. Girgsdies, O. Timpe, E. Rödel,

T. Ressler, A. Trunschke and R. Schlögl, *Top. Catal*, **50**, 19 (2008).
36. S. Royer, D. Duprez and S. Kaliaguine, *Catal. Today*, **112**, 99 (2006).
37. H. X. Dai, C. F. Ng and C. T. Au, *J. Catal.*, **189**, 52 (2000).
38. H. M. Zhang, Y. Shimizu, Y. Teraoka, N. Miura and N. Yamazoe, *J. Catal*., **121**, 432 (1990).
39. S. Kaliaguine, A. Van Neste, V. Szabo, J. E. Gallot, M. Bassir and R. Muzychuk, *Appl. Catal. A*, **209**, 345 (2001).
40. J. M. Wu, H. P. Yang, Y. N. Fan, B. L. Xu and Y. Chen, *J. Fuel Chem. Technol*., **35**, 684 (2007).
41. L. F. Liotta, M. Ousmane, G. Di Carlo, G. Pantaleo, G. Deganello, G. Marcì, L. Retailleau and A. Giroir-Fendler, *Appl. Catal. A*, **347**, 81 (2008).
42. N. Katada, T. Miyamoto, H. A. Begum, N. Naito, M. Niwa, A. Matsumoto and K. Tsutsumi, *J. Phys. Chem. B*, **104**, 5511 (2000).
43. Y. Wang, Q. Zhang, T. Shishido and K. Takehira, *J. Catal.*, **209**, 186 (2002).
44. X. Qinhua and Y. Aizhen, *Prog. Crystal Growth and Charact.*, **21**, 29 (1990).
45. V. N. Romnnnikov, V. M. Mastikhin, S. Hoèevar and B. Držaj, *Zeolite*, **3**, 311 (1983).
46. M. A. Sainz, F. J. Serrano, J. Bastida and A. Caballero, *J. Euro. Ceramic Soc*., **I7**, 1277 (1997).
47. A. H. Boonstra, T. N. M. Bernards and J. J. T. Smits, *J. Non-Cryst. Solids*, **109**, 141 (1989).
48. G. Orcel, L. L. Hench, I. Artaki, J. Jonas and T. W. Zerda, *J. Non-Cryst. Solids*, **105**, 223 (1988).
49. T. Adachi and S. Sakka, *J. Non-Crys. Solids*, **99**, 118 (1988).
50. G. W. Scherer, *J. Non-Cryst. Solids*, **100**, 77 (1988).
51. T. Mizuno, H. Nagata and S. Manabe, *J. Non-Cryst. Solids*, **100**, 236 (1988).
52. X. Tu, N. Furuta, Y. Sumida, M. Takahashi and H. Niiduma, *Catal. Today*, **117**, 259 (2006).
53. P. Korovchenko, N. R. Shiju, A. K. Dozier, U. M. Graham, M. O. Guerrero-Pérez and V. V. Guliants, *Top. Catal*., **50**, 43 (2008).
54. R. K. Grasselli, *Catal. Today*, **49**, 141 (1999).
55. S. S. Kum, B. Y. Jo and S. H. Moon, *Appl. Catal. A*, **365**, 79 (2009).
56. P. Concepción, P. Botella and J. M. L. Nieto, *Appl. Catal. A*, **278**, 45 (2004).
57. M. Baca, A. Pigamo, J. L. Dubois and J. M. M. Millet, *Catal. Comm.*, **6**, 215 (2005).
58. P. Concepción, P. Botella and J. M. López Nieto, *Appl. Catal. A*, **278**, 45 (2004).
59. W. Ueda, D. Vitry and T. Katou, *Catal. Today*, **99**, 43 (2005).
60. D. Linke, D. Wolf, M. Baerns, O. Timpe, R. Schlögl, S. Zeyβ and U. Dingerdissen, *J. Catal.*, **205**, 16 (2002).
61. B. Mitra, I. E. Wachs and G. Deo, *J. Catal.*, **240**, 151 (2006).
62. X. J. Yang, R. M. Feng, W. J. Ji and C. T. Au, *J. Catal.*, **253**, 57 (2008).
63. L. T. Weng and B. Delmon, *Appl. Catal. A*, **81**, 141 (1992).
64. Y. Moro-oka, *Appl. Catal. A*, **181**, 323 (1999).
65. T. Ushikubo, *Catal. Today*, **57**, 339 (2000).
66. D. Vitry, Y. Morikawa, J. L. Dubois and W. Ueda, *Top. Catal*., **23**, 47 (2003).
67. J. Holmberg, R. K. Grasselli and A. Andersson, *Top. Catal*., **23**, 55 (2003).
68. R. K. Grasselli, *Catal. Today*, **99**, 23 (2005).